

## 5.6 THE IMPACT OF DATA INTERACTION ON TARGETED OBSERVATIONS WITH A 4D-VAR DATA ASSIMILATION AND FORECAST SYSTEM

Dacian N. Daescu<sup>1\*</sup>, I. Michael Navon<sup>2</sup>, Santha Akella<sup>3</sup>, Gordon Erlebacher<sup>2</sup>

<sup>1</sup>Portland State University, Portland, Oregon, <sup>2</sup>Florida State University, Tallahassee, Florida,

<sup>3</sup>University of Pennsylvania, Philadelphia, Pennsylvania

### 1. INTRODUCTION

Adaptive observations strategies aim to improve the forecasting skill of numerical weather prediction systems by dynamically identifying optimal locations where additional (targeted) observational data must be collected. Despite many advances in the theoretical formulation and implementation of targeting methods (Palmer et al. 1998, Berliner et al. 1999, Baker and Daley 2000, Bishop et. al 2001, Bergot and Doerenbecher 2002, Leutbecher 2003, Langland and Baker 2004, Majumdar et al. 2006) the problem of the optimal adaptive sampling is a young, dynamically evolving, discipline and many open questions remain to be addressed (Langland, 2005). Optimal deployment of targeted observations requires a systematic assessment of the information provided by the observational network to a specific data assimilation and forecast system. The design of adaptive strategies must account for various factors such as: the forecast model details, the magnitude and the dynamical growth of the uncertainty in the initial conditions, the data assimilation scheme used to provide the initial conditions, the configuration of the conventional observational network (Lorenz and Emanuel 1998, Bergot 2001, Morss et al. 2001).

Targeting methods using total energy singular vectors and analysis sensitivity search for the regions where the forecast is sensitive to analysis errors and provide no guidance on the issues that lie within the realm of data assimilation and not modeling (Baker and Daley 2000). In particular, the interaction between the sampling strategy and other observing systems in the vicinity, as well as the influence of the background error, have not been properly investigated.

The characteristics of the data assimilation system may be integrated in the adaptive observations

method by using the sensitivity to observations technique proposed by Baker and Daley (2000). This approach was developed in the context of 3D-Var data assimilation and was later used for targeting observations by Doerenbecher and Bergot (2001) who emphasized that to optimize the efficiency of adaptive techniques the assimilation of both conventional and adaptive observations must be considered. Langland and Baker (2004) describe an adjoint-based procedure for assessing the impact of observations in a 3D-Var data assimilation and forecast system on a scalar measure of the short-range forecast error.

The issue of data interaction on selecting targeted observations becomes increasingly important in the context of four dimensional variational data assimilation (4D-Var) that allows for multiple time varying targeting areas in the assimilation window following the flow regime. The interaction between time and space distributed adaptive observations and other observing systems in the vicinity is not properly incorporated into current objective targeting methods.

In this work a method to assess the information provided by the routine observational network and to account for data interactions within the targeting procedure is implemented in the 4D-Var context. The method builds on the work of Daescu and Carmichael (2003) and Daescu and Navon (2004) to account for the dynamical interaction between the forecast sensitivity field, as computed with an objective targeting method, and a sensitivity field associated to all additional data available to the assimilation procedure. Numerical results are presented with a 2D global shallow-water model using the Lin-Rood flux-form semi-Lagrangian scheme (Lin and Rood, 1997) and its adjoint. Idealized 4D-Var twin experiments are setup with initial conditions specified from the ECMWF 500mb ERA-40 dataset. A comparative analysis with targeted observations using gradient sensitivity shows that the method to account for data interaction is effective in providing improved forecasts at a low additional computational effort. Limitations of the current implementation and future research directions are also discussed.

---

\*Corresponding author address: Dacian N. Daescu, Department of Mathematics and Statistics, Portland State University, P.O. Box 751, Portland, OR 97207, USA; e-mail: daescu@pdx.edu

## 2. TARGETED OBSERVATIONS IN THE 4D-VAR CONTEXT

The 4D-Var data assimilation searches for an optimal estimate (analysis) to the initial conditions by solving a large-scale optimization problem

$$\min_{\mathbf{x}_0} \mathcal{J}(\mathbf{x}_0); \quad \mathbf{x}_0^a = \text{Arg} \min \mathcal{J} \quad (1)$$

The cost functional

$$\begin{aligned} \mathcal{J} = & \frac{1}{2}(\mathbf{x}_0 - \mathbf{x}_b)^T \mathbf{B}^{-1}(\mathbf{x}_0 - \mathbf{x}_b) \\ & + \frac{1}{2} \sum_{k=1}^N (\mathbf{H}_k \mathbf{x}_k - \mathbf{y}_k)^T \mathbf{R}_k^{-1} (\mathbf{H}_k \mathbf{x}_k - \mathbf{y}_k) \end{aligned} \quad (2)$$

includes the distance to a prior (background) estimate to initial conditions  $\mathbf{x}_b$  and the distance of the model forecast  $\mathbf{x}_k = \mathcal{M}(\mathbf{x}_0)$  to observations  $\mathbf{y}_k, k = 1, 2, \dots, N$  time distributed over the analysis interval  $[t_0, t_N]$ . The model  $\mathcal{M}$  is nonlinear and for simplicity we assume a linear representation of the observational operator  $\mathbf{H}_k$  that maps the state space into the observation space at time  $t_k$ . Statistical information on the errors in the background and data is used to define appropriate weights:  $\mathbf{B}$  is the covariance matrix of the background errors and  $\mathbf{R}_k$  is the covariance matrix of the observational errors. Recent advances in modeling flow-dependent background error variances are discussed by Kucukkaraca and Fisher (2006).

The observational data set  $\mathcal{O} = \{\mathbf{y}\}$  available over the assimilation window has two components  $\mathcal{O} = \mathcal{O}^c \cup \mathcal{O}^a$ , where  $\mathcal{O}^c$  is the set of routine observations provided by the conventional observing network whose location in the time-space domain is assumed to be a priori known and  $\mathcal{O}^a$  is the set of additional (targeted) observations to be included in the 4D-Var procedure. Identification of the targeted observations aims to reduce the error of a forecast aspect at the verification time  $t_v > t_N$  over the verification domain  $\mathcal{D}_v$

$$\mathcal{J}_v(\mathbf{x}_0) = \frac{1}{2} \langle \mathbf{P}(\mathbf{x}_v^f - \mathbf{x}_v^{ref}), \mathbf{P}(\mathbf{x}_v^f - \mathbf{x}_v^{ref}) \rangle_E \quad (3)$$

where  $\mathbf{x}_v^f = \mathcal{M}(\mathbf{x}_0)$ ,  $\mathbf{x}_v^{ref}$  is the verifying analysis at  $t_v$ , and  $\mathbf{P}$  is a diagonal projection operator on  $\mathcal{D}_v$  satisfying  $\mathbf{P}^* \mathbf{P} = \mathbf{P}^2 = \mathbf{P}$ . The inner product  $\langle \cdot, \cdot \rangle_E$  is defined as  $\langle \mathbf{y}, \mathbf{z} \rangle_E = \langle \mathbf{y}, \mathbf{E} \mathbf{z} \rangle$  where  $\mathbf{E}$  is a symmetric positive definite matrix. In practice a total energy norm is often used to measure the forecast error (3). To fully account for the temporal dimension of the 4D-Var scheme multiple targeting instances  $t_0 < t_i \leq t_N, i = 1, \dots, I$  may be considered in

the assimilation window. The targeted observations problem searches for an adaptive observational path  $\mathcal{O}^a = \{\mathcal{O}_1^a, \mathcal{O}_2^a, \dots, \mathcal{O}_I^a\}$  such that the solution  $\mathbf{x}_0^a$  of the corresponding 4D-Var data assimilation (2) minimizes the forecast error expressed by the functional (3). For practical applications (e.g. flight planning) the functional  $\mathcal{J}_v$  must be based on the forecast alone since the forecast error at  $t_v$  is not known at the planning time (Langland et al. 1999). "A posteriori" ("after-the-fact") studies provide valuable insight on the benefits and shortcomings of targeted observations and in this case  $\mathcal{J}_v$  is taken to be the forecast error at  $t_v$  measured by the functional (3).

### 2.1 Adjoint-based sensitivity methods

Singular vectors and gradient sensitivity are targeting methods that rely on the linearization of the nonlinear forecast model and tangent linear and adjoint model integrations. To first order approximation, a perturbation  $\delta \mathbf{x}_i$  in the model state at  $t_i$  evolves to optimization time  $t_v$  into

$$\delta \mathbf{x}_v = \mathcal{M}(\mathbf{x}_i + \delta \mathbf{x}_i) - \mathcal{M}(\mathbf{x}_i) \approx \mathbf{M}(t_i, t_v) \delta \mathbf{x}_i \quad (4)$$

$$\delta \mathcal{J}_v \approx \langle \nabla_{\mathbf{x}_v} \mathcal{J}_v, \delta \mathbf{x}_v \rangle = \langle \mathbf{M}^*(t_v, t_i) \nabla_{\mathbf{x}_v} \mathcal{J}_v, \delta \mathbf{x}_i \rangle \quad (5)$$

where  $\mathbf{M}(t_i, t_v)$  is the resolvent of the tangent linear model in the optimization interval  $t_v - t_i$  and  $\mathbf{M}^*(t_v, t_i)$  its adjoint model. For the discrete dynamics, the adjoint  $\mathbf{M}^*$  is simply the transpose matrix  $\mathbf{M}^T$ . A sensitivity function  $F_{v,i}(\lambda, \theta)$  is used to identify regions where errors in the analysis at the targeting time  $t_i$  will have most impact on the forecast at  $t_v$  over  $\mathcal{D}_v$ .

In the adjoint sensitivity approach targeted observations are selected using the gradient of the functional  $\mathcal{J}_v$  defined in terms of the forecast at the verification time. Ideally, we would like to evaluate the sensitivity of the forecast error (3) with respect to the model state at the targeting time. A large sensitivity value indicates that small variations in the model state will have a significant impact on the forecast at the verification time. The sensitivity field at longitude-latitude grid location  $(\lambda, \theta)$  is defined as

$$F_{v,i}(\lambda, \theta) = \|\mathbf{M}^*(t_v, t_i) \nabla_{\mathbf{x}_v} \mathcal{J}_v\|_{(\lambda, \theta)} \quad (6)$$

(vertically integrated gradient norm) and targeted observations at  $t_i$  are deployed at locations  $(\lambda, \theta)$  where  $F_{v,i}(\lambda, \theta)$  has largest values. Identification of the target area at distinct instants in time proceeds backward from  $t_I$  to  $t_1$  and an efficient evaluation of all  $\nabla \mathcal{J}_v(\mathbf{x}_i), i = 1, 2, \dots, I$  is obtained through a single adjoint model integration. The adjoint sensitivity method may be therefore implemented at a

reduced computational cost even in the case when multiple targeting instants are considered.

The singular vectors approach to targeting observations (Palmer et al. 1998, Buizza and Montani 1999) is computationally intensive since the leading eigenvectors are obtained by solving the generalized eigenvalue problem

$$(\mathbf{PM})^* \mathbf{E} (\mathbf{PM}) \boldsymbol{\nu} = \sigma^2 \mathbf{A}^{-1} \boldsymbol{\nu} \quad (7)$$

in the optimization interval  $t_v - t_i$ . The specification of the metrics  $\mathbf{E}$  and  $\mathbf{A}^{-1}$  at time  $t_v$  and  $t_i$ , respectively is discussed by Palmer et al. (1998). An optimal choice for  $\mathbf{A}$  is the analysis error covariance matrix that may be approximated by the inverse Hessian matrix of the cost functional in the 4D-Var. The use of Hessian singular vectors (HSV) in a 3D-Var context is discussed by Barkmeijer et al. (1999). The total energy singular vectors (TESV) are obtained by selecting the total energy metric at the targeting time  $t_i$  and at the verification time  $t_v$ ,  $\mathbf{A}^{-1} = \mathbf{E}$ . The computational burden of (7) is thus reduced since  $\mathbf{E}$  is a diagonal matrix. The sensitivity function is defined using the first  $m$ -leading TESV  $\boldsymbol{\nu}_j$  with unit  $\mathbf{E}$ -norm

$$F_{v,i}(\lambda, \theta) = \sum_{j=1}^m (\sigma_j^2 / \sigma_1^2) f_j(\lambda, \theta) \quad (8)$$

where  $f_j(\lambda, \theta)$  denotes the (vertically integrated) total energy of  $\boldsymbol{\nu}_j$  at grid point  $(\lambda, \theta)$  and targeted observations are taken at the locations  $(\lambda, \theta)$  where  $F_{v,i}(\lambda, \theta)$  takes the largest values. The computational cost of implementing targeting methods using singular vectors is significantly increased when multiple targeting instants are considered since for each  $t_i, i = 1, 2, \dots, I$  a new set of singular vectors must be computed.

## 2.2 The impact of data interaction

Baker and Daley (2000) noticed that the optimality criteria of objective targeting methods based on TESV and adjoint sensitivity does not properly account for the characteristics of the data assimilation system (DAS). Targeted observations at instant  $t_i$  are selected assuming that these are *the only* available observations and the impact of other observing systems in the vicinity is neglected. Since the 4D-Var data assimilation takes into consideration *all* observations available in the assimilation window, the impact of data interaction must be considered by the targeting procedure. Sensitivity to observations techniques have been considered in the 3D-Var context to assess the impact of targeted observations in

the presence of data from the routine observational network (Doerenbecher and Bergot 2001, Bergot and Doerenbecher 2002, Langland and Baker 2004) and an extension to the 4D-Var data assimilation scheme is yet to be implemented.

The use of influence functions associated to the observations was considered by Daescu and Carmichael (2003) and Daescu and Navon (2004) as a cost-effective approach to assess the interaction between targeted and routine observations. The influence function associated to observations  $\mathbf{y}_k$  at time  $t_k$  is defined for  $t_i \leq t_k$  as the gradient norm

$$F_{k,i}(\lambda, \theta) = \|\mathbf{M}^*(t_k, t_i) \nabla_{\mathbf{x}_k} \mathcal{J}(\mathbf{x}_k)\|_{(\lambda, \theta)} \quad (9)$$

of the 4D-Var cost functional  $\mathcal{J}$  restricted to the observational set  $\mathbf{y}_k$ . A large value of the influence function  $F_{k,i}$  indicates that information provided by observational data  $\mathbf{y}_k$  has a significant impact in determining the analysis at  $t_i$ . To account for data interaction, the forecast error sensitivity field  $F_{v,i}$  is updated at  $t_i$  according to

$$F_{v,i}(\lambda, \theta) = F_{v,i}(\lambda, \theta) \left( 1 + \alpha \frac{F_{k,i}(\lambda, \theta)}{F_{v,i}(\lambda, \theta)} \right)^{-1} \quad (10)$$

The updated sensitivity field is inversely proportional to the relative value of the influence function associated to the set of observations that have been already located such as routine observations. Targeted observations at  $t_i$  are located in regions where the forecast sensitivity  $F_{v,i}$  to analysis errors is large *and* little additional information may be extracted from all other observational resources. The interaction between observations is controlled by the weight coefficient  $\alpha > 0$  which reflects the confidence in the previously selected observations (e.g. observational errors). Using this procedure the redundancy between time distributed targeted and routine observations is minimized. The computational overhead required by the updating procedure (10) is roughly given by the computational cost of a adjoint model integration in the 4D-Var assimilation window  $[t_0, t_N]$ . The additional computational effort is thus low and numerical experiments indicate that the procedure is effective in selecting targeted observations that provide improved forecasts.

## 3. NUMERICAL EXPERIMENTS

The numerical experiments are performed with a two-dimensional global shallow-water (SW) model using the explicit flux-form semi-Lagrangian (FFSL) scheme of Lin and Rood (1997) at a  $2.5^\circ \times 2.5^\circ$  resolution and a constant time step  $\Delta t = 450$  s. As

a reference initial state  $\mathbf{x}_0^{ref}$  we consider the 500mb ECMWF ERA-40 data valid for March 15, 2002 06h. 4D-Var data assimilation experiments are setup in a twin experiments framework using as background estimate  $\mathbf{x}_b$  to the initial conditions the 500mb ECMWF ERA-40 data valid for March 15, 2002 00h, six hours prior to the reference state  $\mathbf{x}^{ref}$ . The 24h forecast error  $\mathbf{x}_v^{ref} - \mathbf{x}_v^f = \mathcal{M}(\mathbf{x}_0^{ref}) - \mathcal{M}(\mathbf{x}_b)$  in a total energy metric exhibits a large magnitude over the region  $\mathcal{D}_v = [55^\circ W, 35^\circ W] \times [52^\circ N, 65^\circ N]$  that is defined as the verification domain at  $t_v = 24$ h. The configuration of the geopotential height for the reference initial state and the 24h forecast error over the verification domain are displayed in Figure 1.

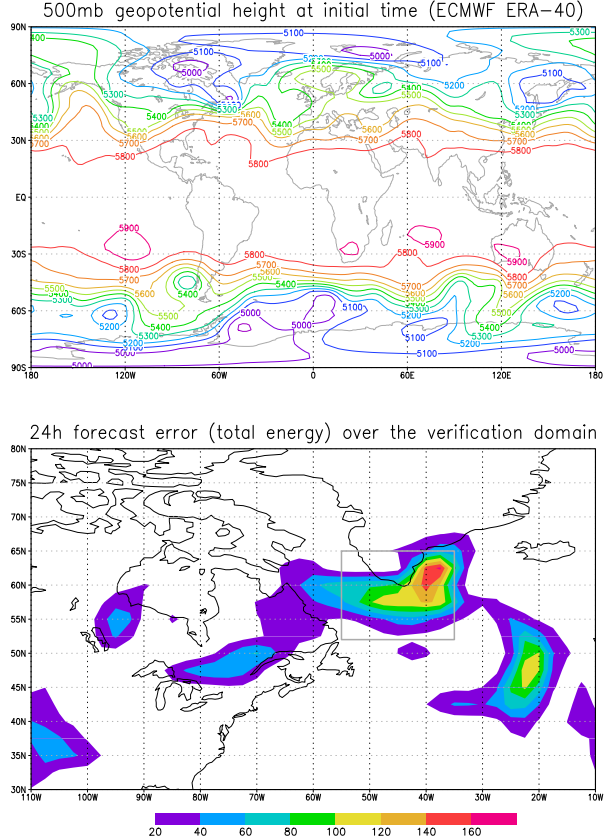


Figure 1: Reference geopotential height at the initial time and the error over the verification domain of a 24h forecast initiated from the background estimate.

For the 4D-Var experiments a six hours 0-6h data assimilation time interval is considered. Model generated data from a reference run is used to simulate a routine observational network that provides "observational data"  $\mathcal{O}^c$  at every 4<sup>th</sup> grid point on the longitudinal and latitudinal directions at  $t_N = 6$ h ( $\sim 6\%$  of the state is "observed"). The data as-

similation system that incorporates only the routine observations is hereafter referred to as DAS-I. The targeting instant is taken at  $t=0$ h, where a number of 20 targeted observations must be selected. For a total energy forecast aspect  $\mathcal{J}_v$ , the target area identified by the gradient sensitivity method (6) was found to be nearly identical to the target area identified by 20 leading total energy singular vectors (8), as shown in Figure 2.

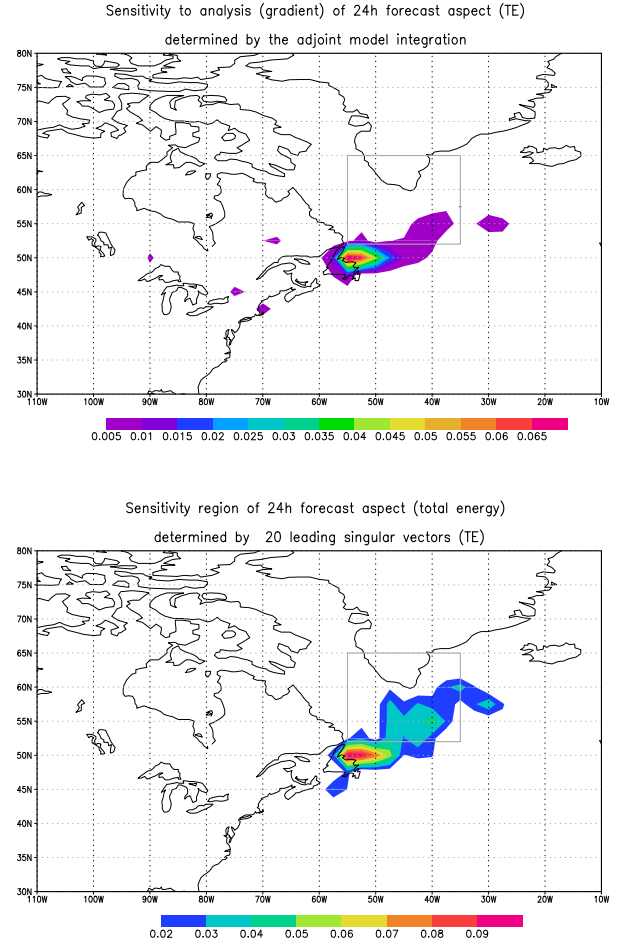


Figure 2: Target area at  $t=0$ h identified by the gradient of the total energy forecast (top) and by the total energy singular vectors (bottom).

### 3.1 Observation targeting experiments

The twin experiments setup allows for "a posteriori" targeting experiments with the functional  $\mathcal{J}_v$  defined to be the forecast error at  $t_v$ . The corresponding sensitivity field (6) identified by the adjoint sensitivity method and the location of targeted observations (leading 5) is displayed in Figure 3. In this case the selection of targeted observations does not account for the impact of routine data, and

the corresponding DAS is hereafter referred to as DAS-II.

coefficient  $\alpha = 1$ . The corresponding DAS includes targeted observations that account for the impact of routine data and is hereafter referred to as DAS-III.

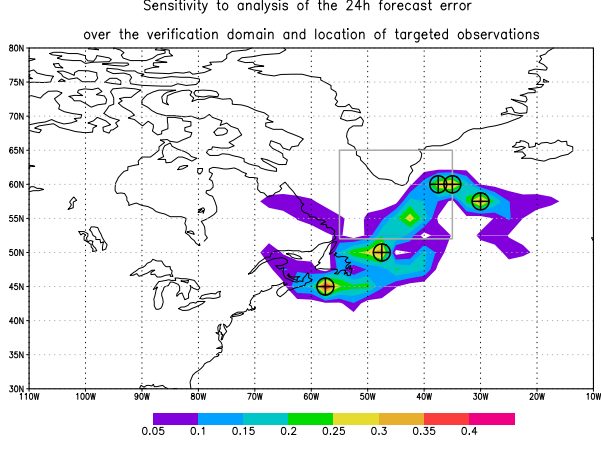


Figure 3: Targeted observations at  $t=0$ h identified by the gradient of the total energy forecast error, without taking into account interaction with data at  $t=6$ h.

To assess the impact of the routine observations at the targeting time, the influence field (9) associated to the routine observations is computed using an additional adjoint model integration from  $t=6$ h to  $t=0$ h as displayed in Figure 4.

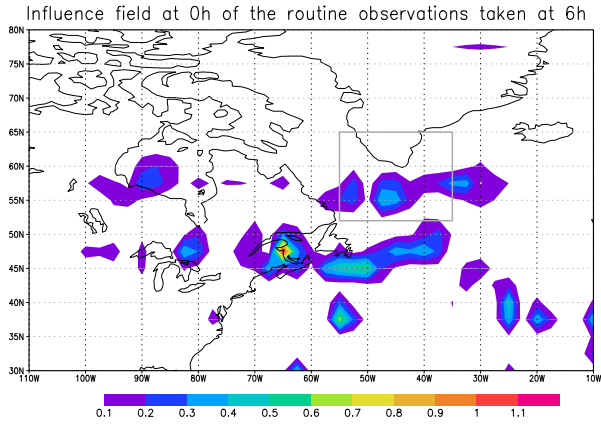


Figure 4: The influence function at  $t = 0$ h associated to the routine observations taken at  $t = 6$ h.

The interaction between the forecast error sensitivity field and the observation influence field is illustrated in Figure 5 and is taken into account in the observation targeting procedure by performing the update (10). The updated sensitivity field (10) and the new location of the targeted observations (leading 5) are also displayed in Figure 5 for a weight

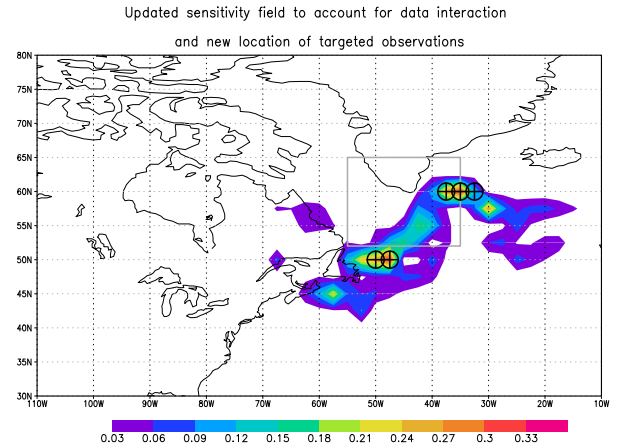
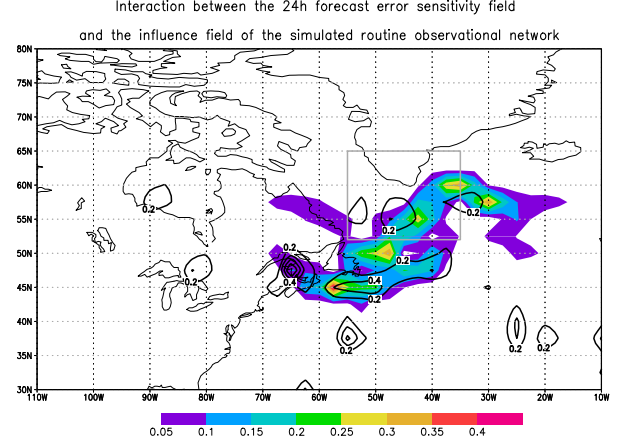


Figure 5: Top: Interaction between the forecast error sensitivity field and influence field associated to the routine observations. Bottom: Updated sensitivity field and location of targeted observations to account for data at  $t = 6$ h.

### 3.2 Data assimilation results

Data assimilation experiments that differ only in the selection of the observational data set included in the optimization cost functional are performed for each of the DAS-I, DAS-II, and DAS-III configurations. The error in the forecast  $\mathbf{x}_v^f = \mathcal{M}(\mathbf{x}_0^\alpha)$  provided by each DAS is displayed in Figure 6 and Figure 7 as mean values of the grid point energy errors averaged over the longitudinal and latitudinal

directions, respectively.

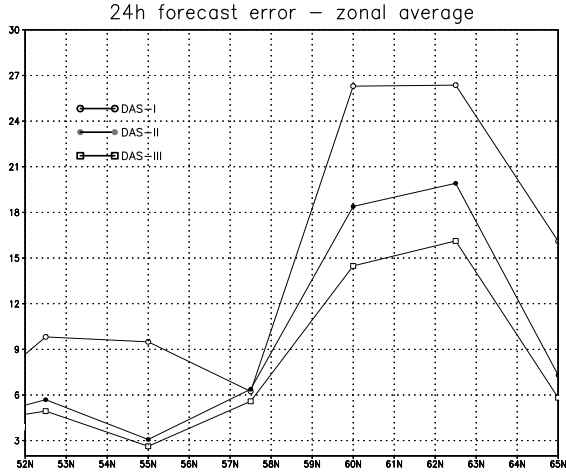


Figure 6: Zonal-average forecast error over the verification domain provided by the 4D-Var data assimilation with each of DAS-I, DAS-II, DAS-III.

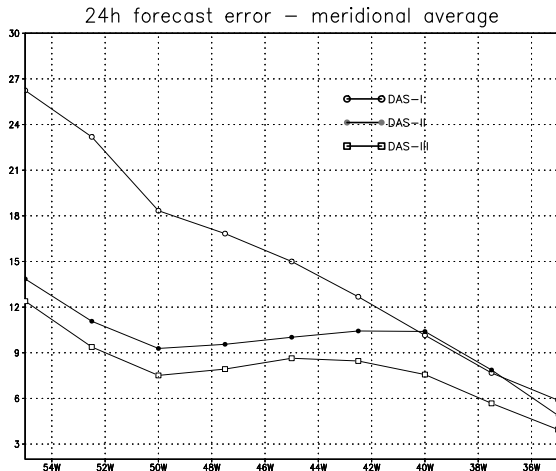


Figure 7: Meridional-average forecast error over the verification domain provided by the 4D-Var data assimilation with each of DAS-I, DAS-II, DAS-III.

The DAS-I forecast is based on the assimilation of routine observations only and it is noticed that the insertion of the targeted observations in DAS-II provided a significantly improved forecast. Accounting for data interaction between routine and targeted observations in DAS-III provided further improvement and in certain regions a reduction by as much as  $\sim 25\%$  in the forecast error versus DAS-II. In Figure 7 one notice that accounting for data interaction in DAS-III is of particular benefit to the forecast in the verification region  $42^{\circ}W - 36^{\circ}W$  where DAS-II

provides little or no benefit over DAS-I.

### 3.3 Conclusions

In this study it is shown that the interaction between targeted observations and the routine observational network has a significant impact on the efficiency of the adaptive strategies. A cost-effective data interaction mechanism based on adjoint sensitivities is implemented to identify regions where the sensitivity of the forecast to the analysis errors is large and little additional information may be obtained from other observational resources. A rigorous theoretical framework to account for multiple targeting instants and the interaction between time distributed targeted observations remains to be formulated. A formal extension of the 3D-Var sensitivity to observations to the 4D-Var data assimilation is necessary to analyze the interaction between the existing observational network, the background estimate of the model state, and adaptive observations.

### Acknowledgements

This research was supported by NASA Modeling, Analysis and Prediction Program under award No. NNG06GC67G.

### References

- Baker, N.L., and R. Daley, 2000: Observation and background adjoint sensitivity in the adaptive observation-targeting problem. *Q.J.R. Meteorol. Soc.*, **126**, 1431–1454.
- Barkmeijer, J., Buizza, R., and T.N. Palmer, 1999: 3D-Var Hessian singular vectors and their potential use in the ECMWF Ensemble Prediction System. *Q.J.R. Meteorol. Soc.*, **125**, 2333–2351.
- Bergot, T., and A. Doerenbecher, 2002: A study on the optimization of the deployment of targeted observations using adjoint-based methods. *Q.J.R. Meteorol. Soc.*, **128**, 1689–1712.
- Bergot, T., 2001: Influence of the assimilation scheme on the efficiency of adaptive observations. *Q.J.R. Meteorol. Soc.*, **127**, 635–660.
- Berliner, L.M., Lu, Z.Q., and C. Snyder, 1999: Statistical design for adaptive weather observations. *J. Atmos. Sci.*, **56**, 2536–2552.
- Bishop, C.H., Etherton, B.J., and S.J. Majumdar, 2001: Adaptive sampling with the ensemble transform Kalman filter. Part I: Theoretical aspects. *Mon. Wea. Rev.*, **129**, 420–436.
- Buizza, R., and A. Montani, 1999: Targeted obser-

vations using singular vectors. *J. Atmos. Sci.*, **56**, 2965–2985.

Daescu, D.N., and I.M. Navon, 2004: Adaptive observations in the context of 4D-Var data assimilation. *Meteorol. Atmos. Phys.*, **85**, 205–226.

Daescu, D.N., and G.R. Carmichael, 2003: An adjoint sensitivity method for the adaptive location of the observations in air quality modeling. *J. Atmos. Sci.*, **60** (2), 434–450.

Doerenbecher, A., and T. Bergot, 2001: Sensitivity to observations applied to FASTEX cases. *Non. Proc. Geophys.*, **8**, 467–481.

Kucukkaraca, E. and M. Fisher, 2006: Use of analysis ensembles in estimating flow-dependent background error variances. *ECMWF Technical Memorandum*, **492**. European Centre for Medium-range Weather Forecasts (ECMWF), Reading, UK.

Langland, R.H., 2005: Issues in targeted observing. *Q.J.R. Meteorol. Soc.*, **131**, 3409–3425.

Langland, R.H., and N.L. Baker, 2004: Estimation of observation impact using the NRL atmospheric variational data assimilation adjoint system. *Tellus*, **56A**, 189–203.

Langland, R.H., Gelaro, R., Rohaly, G.D., and M.A. Shapiro, 1999: Targeted observations in FASTEX: Adjoint-based targeting procedures and data impact experiments in IOP17 and IOP18. *Q.J.R. Meteorol. Soc.*, **125**, 3241–3270.

Leutbecher, M., 2003: A reduced rank estimate of forecast error variance changes due to intermittent modifications of the observing network. *J. Atmos. Sci.*, **60**, 729–742.

Lin, S.-J., and R.B. Rood, 1997: An explicit flux-form semi-Lagrangian shallow-water model on the sphere. *Q.J.R. Meteorol. Soc.*, **123**, 2477–2498.

Lorenz, E.N., and K.A. Emanuel, 1998: Optimal sites for supplementary weather observations: simulation with a small model. *J. Atmos. Sci.*, **55**, 399–414.

Majumdar, S.J., Aberson, S.D., Bishop, C.H., Buizza, R., Peng, M.S., and C.A. Reynolds, 2006: A comparison of adaptive observing guidance for Atlantic tropical cyclones. *Mon. Wea. Rev.*, **134**, 2354–2372.

Morss, R.E., Emanuel, K.A., and C. Snyder, 2001: Idealized adaptive observation strategies for improving numerical weather prediction. *J. Atmos. Sci.*, **58** 210–234.

Palmer, T.N., Gelaro, R., Barkmeijer, J., and R. Buizza, 1998: Singular vectors, metrics, and adaptive observations. *J. Atmos. Sci.*, **55**, 633–653.